

Acetate Facilitated Nickel Catalyzed Coupling of Aryl Chlorides and Alkyl Thiols

Regina M. Oechsner, J. Philipp Wagner,* and Ivana Fleischer*

Institute of Organic Chemistry, Faculty of Mathematics and Natural Sciences, Eberhard Karls University Tübingen, Auf der Morgenstelle 18, 72076 Tübingen, Germany, E-mail: ivana.fleischer@uni-tuebingen.de

ABSTRACT: We report a mild, fast and convenient catalytic system for the coupling of aryl chlorides with primary, secondary, as well as previously challenging tertiary alkyl thiols using an air-stable nickel(II) precatalyst in combination with the low-cost base potassium acetate at room temperature. This new catalytic system tolerates a variety of functional groups and enables the generation of thioethers for a wide range of substrates, including pharmaceutical compounds in excellent yields. Chemoselective functionalization of disubstituted substrates was demonstrated. Kinetic and NMR-studies, as well as DFT computations support a Ni(0)/Ni(II) catalytic cycle and identify the oxidative addition product as the resting state. Acetate coordination and subsequent acetate facilitated formation of a thiolate complex via internal deprotonation play a key role in the catalytic cycle.

INTRODUCTION

The metal catalyzed C-S cross-coupling of aryl (pseudo)halides and thiols under basic conditions, known as Migita reaction, provides an efficient access to thioethers.¹ The more lipophilic bioisosters of ethers are an attractive structural motif in pharmaceutical compounds, agrochemicals and materials design.² Most academic research in the past focused on palladium catalyzed reactions³ and the same was true for industrial applications,⁴ but low-cost nickel-catalysts can replace the precious metal. This, as well as its intriguing and versatile reactivity patterns,⁵ are the reason why nickel has evolved into an intensively researched and popular metal for homogeneous catalysis.

While most nickel-catalyzed C-S couplings were developed for the transformation of more reactive aryl bromides and iodides,⁶ the reactions of aryl chlorides remained rare until recently (Scheme 1a).⁷ Aryl chlorides are comparatively more challenging to couple, but they are readily accessible compounds with a vast range of commercially available substrates, which renders them invaluable for organic synthesis. Apart from few exceptions such as the trifluorothiomethylation by Schoenebeck and co-workers,^{7b} the scope of nickel-catalyzed couplings of aryl chlorides is often limited, higher catalyst loadings and temperatures, stoichiometric additives or sensitive organometallic bases are required. The latter was also the case in our report on the coupling of aryl chlorides with thiols in the presence of organomagnesium or -zinc reagents as bases and activating agents.⁸ Primary and secondary alkyl thiols were coupled efficiently, but tertiary thiols reacted with low yields.

The coupling of tertiary thiols remains a challenge in nickel catalysis, regardless of the employed coupling partner.⁹ It is performed under harsh conditions in most cases and typically, only few substrates are shown, without systematic investigation. Notable exceptions are the recent report on the coupling of aryl bromides with a Ni-diimine catalyst, by Stefan

and co-workers,^{9k} and the work by Morandi and co-workers on metathesis of thioanisols.⁹ⁱ

Nevertheless, to the best of our knowledge, there is no published efficient coupling of aryl chlorides and tertiary alkyl thiols with high yields under mild reaction conditions. Therefore, our goal was to develop a general method for the nickel-catalyzed coupling of aryl chlorides with primary, secondary and especially tertiary aliphatic thiols. We achieved this by employing the precatalyst (Xantphos)Ni(*o*-tolyl)Cl (**C1**; Xantphos = (9,9-Dimethyl-9H-xanthene-4,5-diyl)bis(diphenylphosphane)), first reported by Jamison¹⁰ as air-stable, easily synthesized Ni(II) precursor,¹¹ together with potassium acetate as low-cost and air stable base at room temperature (Scheme 1b). We present the results of our investigation on the substrate scope together with mechanistic studies, which uncovered the role of acetate in the catalytic cycle.

Scheme 1. Current challenges for the nickel-catalyzed C-S cross-coupling and our approach to tackle them

a) General: Ni-Catalyzed C-S Coupling - Challenges



Challenge 1:

ArCl as substrate

- high BDE of C-Cl bond
- less reactive
- but available and cheap

Challenge 2:

aliphatic 3° thiols

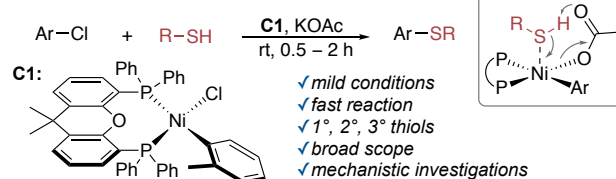
- often low yields
- side reactions
- unexplored

Challenge 3:

reaction conditions

- high-cost
- high temperature
- long reaction time

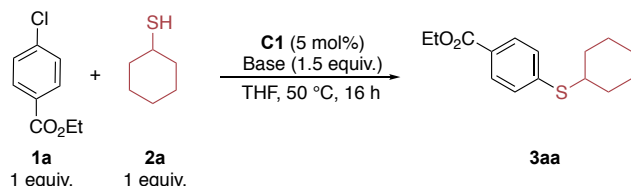
b) This Work: Acetate = Key to Success



RESULTS AND DISCUSSION

We began our investigation with the overall goal to find a simple and economical catalytic system to render air-sensitive transmetalation reagents and high temperatures redundant, by using precatalyst **C1** and examining various bases (Table 1 and Table S1 in the SI). At first, the easier to couple secondary cyclohexanethiol (**2a**) and aryl chloride **1a** were tested. To our surprise, a large variety of screened bases were successful in the cross-coupling at 50 °C, generating thioether **3aa** in low to moderate yields (entries 1-11). Sodium acetate could be identified as suitable base for the C-S cross-coupling providing a high yield of **3aa** (entry 12).

Table 1. Base screening for the coupling of the aryl chloride 1a with cyclohexanethiol 2a^a



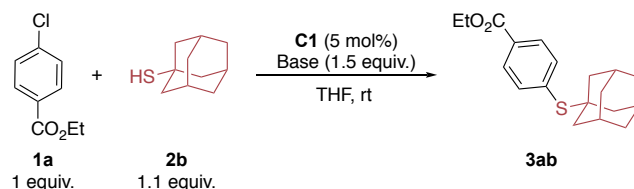
| entry | base | conversion (%) ^b | yield (%) ^b |
|-------|---|-----------------------------|------------------------|
| 1 | NaO ^t Bu | 98 | 19 |
| 2 | Li ₂ CO ₃ | 13 | 10 |
| 3 | Na ₂ CO ₃ | 60 | 56 |
| 4 | K ₂ CO ₃ | 56 | 52 |
| 5 | Cs ₂ CO ₃ | 12 | 9 |
| 6 | Zn ₅ (CO ₃) ₂ (OH) ₆ | 68 | 66 |
| 7 | Zn(OPiv) ₂ | 34 | 33 |
| 8 | Zn(OAc) ₂ | 60 | 54 |
| 9 | Na ₄ P ₂ O ₇ | 6 | 4 |
| 10 | Na ₂ HPO ₄ | 65 | 62 |
| 11 | Sodium citrate | 44 | 42 |
| 12 | NaOAc | 89 | 85 |

^aReaction conditions: ethyl 4-chlorobenzoate (350 μmol, 1.0 equiv.), cyclohexanethiol (350 μmol, 1.0 equiv.), base (1.5 equiv.), **C1** (5 mol%), THF (1 mL), 50 °C, 16 h. ^bGC-FID yields using pentadecane as internal standard.

Intrigued by the efficiency of sodium acetate we continued screening different counterions in the arylation of the more challenging adamantanethiol (**2b**) at room temperature (Table 2). While no or low reactivity was observed after 2 h using lithium and sodium acetates (entries 1, 3), potassium and caesium acetates showed excellent performance (entries 5, 6). A prolonged reaction time of 16 h led to increased yield with sodium acetate, while lithium acetate still performed poorly (entries 2, 4). Low-cost potassium acetate was chosen as optimal base over the caesium salt for further optimization of the reaction conditions (temperature, catalyst loading and substrate equivalents; see SI tables S2-S4). Upon optimization, 1 equiv. of aryl halide, 1.1 equiv. of thiol, 5 mol% **C1**,

1.5 equiv. of KOAc in THF at room temperature were identified as ideal reaction conditions.

Table 2. Comparison of acetates in the coupling of the aryl chloride 1a with tertiary thiol 2b^a



| entry | base | time (h) | conversion (%) ^b | yield (%) ^b |
|-------|-------|----------|-----------------------------|------------------------|
| 1 | LiOAc | 2 | 4 | 0 |
| 2 | LiOAc | 16 | 5 | 2 |
| 3 | NaOAc | 2 | 20 | 14 |
| 4 | NaOAc | 16 | 86 | 83 |
| 5 | KOAc | 2 | 95 | 95 |
| 6 | CsOAc | 2 | 95 | 93 |

^aReaction conditions: ethyl 4-chlorobenzoate (350 μmol, 1.0 equiv.), adamantanethiol (385 μmol, 1.1 equiv.), acetate (1.5 equiv.), **C1** (5 mol%), THF (1 mL), rt. ^bGC-FID yields using pentadecane as internal standard.

Subsequently, the substrate scope as well as functional group tolerance were explored with potassium acetate under optimized conditions. First, adamantanethiol was used as benchmark substrate to test a variety of aryl chlorides (Table 3). A wide range of electron-neutral, electron-rich and electron-deficient *meta*- and *para*-substituted aryl chloride derivatives could be coupled in good to excellent yields. Various functional groups like ethers **3eb**, ketones **3fb**, esters **3ab**, amides **3jb** and nitriles **3nb** were tolerated. The sulfone **4cb** was obtained after oxidation of **3cb** with *m*-CPBA. For *ortho*-substituents, only low yields of **3rb** could be obtained (15%) by employing the aryl chloride, whereas the bromide was converted in excellent yield (87%), showcasing the more facile oxidative addition. The low reactivity of chloride **1r** was used for a selective functionalization of dichloride **1s** to furnish monothioether **3sb** by steric discrimination.

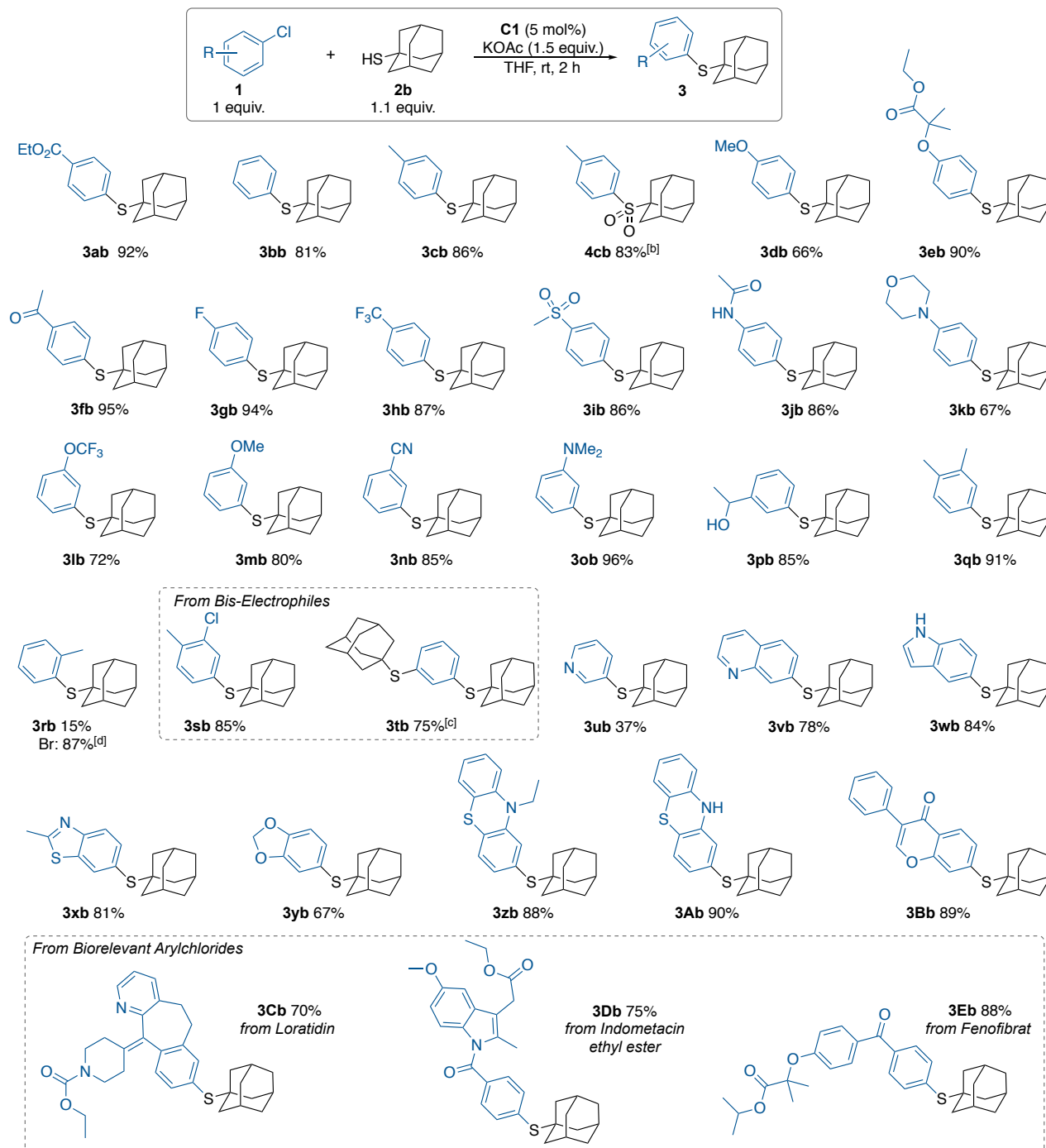
Heterocycles, which are important motifs in pharmaceuticals and agrochemicals, like pyridine, quinoline, indole, thiazole, dioxole, phenothiazine or 4*H*-chromen-4-one were tolerated and afforded the corresponding products **3ub-Bb** in good to excellent yields. Moreover, the successful sulfenylation of pharmaceutically active compounds or their derivatives like Loratidin (**3Cb**, allergy medication), Indometacine ethyl ester (**3Db**, anti-inflammatory drug) and Fenofibrat (**3Eb**, a drug against cardiovascular disease) demonstrates the potential of this reaction for the derivatization of bioactive molecules and highlights the scope and applicability of the methodology in a pharmaceutical context. Notable limitations are aldehyde, acid or primary amine functionalities (see SI).

The substrate scope with regards to the thiol was evaluated next, with a focus on the previously challenging tertiary thiols (Table 4). Ethyl-4-chlorobenzoate (**1a**) was used as standard electrophile. Primary, secondary and a variety of sterically challenging tertiary alkyl thiols were coupled providing the

desired thioether in good to excellent yields. Functional groups such as ketone **3al**, **3am** and ester **3an** were tolerated. Thiocholesterol as a large, bioactive model thiol could be converted to **3ap** in 72% yield. Moieties like amines and acid groups as well as aryl, benzyl and homobenzyl thiols were not

tolerated so far. The inhibition by thiols containing an aryl moiety in certain distances from the sulfur atom might be explained by a bidentate coordination of these compounds, since arenes can act as ligands for Ni(0) species.¹²

Table 3. Substrate scope with respect to aryl chlorides^a

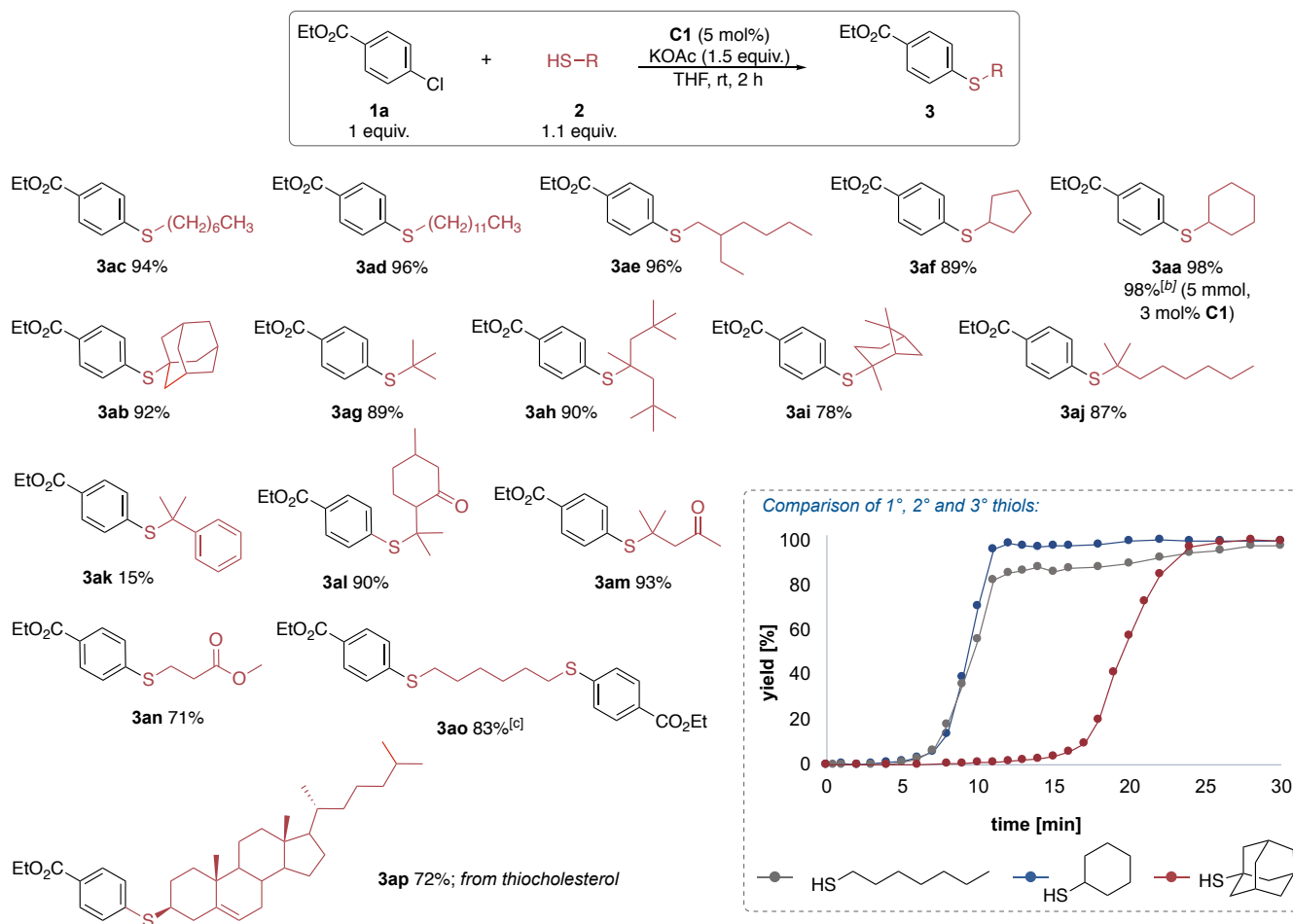


^aStandard reaction conditions: **1** (1.0 equiv.), **2b** (1.1 equiv.), KOAc (1.5 equiv.), **C1** (5 mol%), THF (3 mL), rt, 2 h. Yields of isolated products unless stated otherwise. ^bIsolated as sulfone after oxidation with *m*-CPBA (yield over two steps). ^cWith 2.1 equiv. of **2b**. ^dGC-FID yields using pentadecane as internal standard.

Comparison of the reaction progress for representatives of primary (heptane-), secondary (cyclohexane-) and tertiary (adamantane-) thiols showed similar reaction rates but a significantly longer induction period for the tertiary

adamantanethiol (1°, 2° ≈ 5 min ; 3° ≈ 15 min, Table 4). This period might arise from the involvement of the thiol in the activation of **C1**, which will be discussed later.

Table 4. Substrate scope with respect to alkyl thiols^a



^aStandard reaction conditions: **1a** (1.0 equiv.), **2** (1.1 equiv.), KOAc (1.5 equiv.), **C1** (5 mol%), THF (3 mL), rt, 2h. Yields of isolated products unless stated otherwise. ^b5 mmol, **C1** (3 mol%), rt, 30 min. ^cWith 2 equiv. of **1a**.

Air stability and low cost of the reaction components are advantageous for the newly developed system. The reaction is operationally simple, and solids can be weighed under benchtop conditions before using inert conditions during the reaction. The coupling is fast (30 min – 2 h) and takes place at room temperature. Upscaling of the reaction in the synthesis of **3aa** while lowering the catalyst loading (5 mmol, 3 mol% **Cl**, 30 min), as well as the ability to couple pharmaceutical compounds in good to excellent yields render this method interesting for possible industrial use. Another advantage is the high selectivity with little to no side reactions. Conversion and yield correlate for most substrates with max. 5% difference and for unsuccessful reactions, the substrates could mostly be isolated and reused.

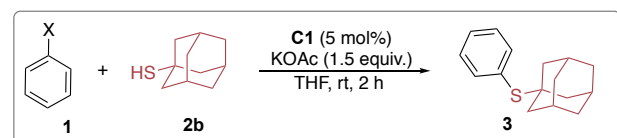
The identified reaction conditions are versatile and can be applied to a variety of electrophiles in addition to aryl chlorides. Phenyl bromide, iodide as well as triflate reacted in excellent yields (Scheme 2a). Interestingly, tosylates performed poorly. To assess the reactivity in greater detail, we subsequently undertook inter- and intramolecular competition experiments comparing the reactivity of different C-X (X = Cl, Br, I, OTf, OTs) bonds. Intermolecular competition experiments between the electrophiles showed that every electrophile except tosylate reacted preferably to phenyl chloride, with the order $\text{PhOTf} >$

PhBr > PhI > PhCl when yields were compared after 2 h (Scheme 2b).

The reaction profiles of different electrophiles (Scheme 2c) showed an increase of the induction period from PhOTf < PhI < PhBr < PhCl and the reaction rate decreasing as followed: PhOTf > PhBr > PhCl > PhI, with phenyliodide as unexpected exception. Otherwise, the results roughly correlate with the expected ease of oxidative addition. The lower reactivity of PhI could be explained with Schoenebeck's¹³ observation that for nickel-catalyzed reactions with aryl iodides more off cycle Ni(I) species are formed and the catalysis is slower.

Intrigued by the intermolecular selectivity and inspired by literature reports on chemoselective Pd¹⁴ and Ni-catalyzed¹⁵ couplings, we decided to examine if related transformations are possible with our system. Introducing substrates with two or more (pseudo)halide functionalities can enable selective, sequential reactions to generate complex functionalized target compounds or products with an intact and reactive functional group. Therefore, several 1,4-dielectrophilic substrates were subjected to intramolecular competition experiments (Scheme 3a).

Scheme 2. Reactivity of electrophiles and intermolecular competition experiments^a



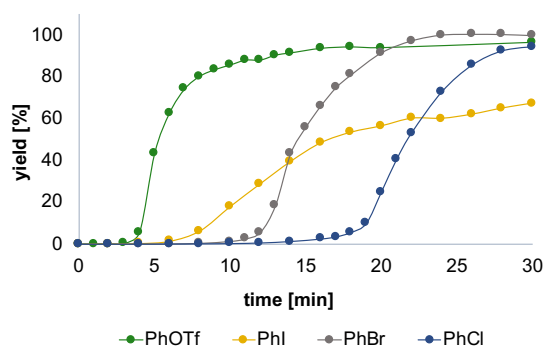
a) Comparison of electrophiles (1 equiv. of **1** (Y = H) + 1.1 equiv. of **2b**)

| | | | | | |
|-----------------|-----|-----|-----|-----|-----|
| | | | | | |
| GC yield: | 94% | 99% | 91% | 99% | <5% |
| Isolated yield: | 81% | 89% | 95% | 96% | |

b) Intermolecular competition (1 equiv. of **1-1** (Y = H) + 1 equiv. of **1-2** (X = H) + 1.1 equiv. of **2b**)

| | | | | | | | | |
|-----------|----|-----|----|-----|----|-----|-----|----|
| | | | | | | | | |
| GC conv.: | 9% | 95% | 1% | 95% | 0% | 92% | 98% | 0% |

c) Reaction progress



^aGC-FID yields with pentadecane as internal standard.

No significant selectivity for monofunctionalization was observed between two different halides C-Cl vs. C-Cl, C-Br and C-I. The difference in reactivity was not sufficient enough under standard conditions, although the more reactive C-X bond was functionalized preferentially (only **3-X** as monosubstituted product, no **3-Y** can be observed), following the typical reactivity order of arylhalides toward oxidative addition with $\text{ArI} > \text{ArBr} > \text{ArCl}$. Unfortunately, the difunctionalized product **3-XY** was obtained as well, explaining the lower conversion of electrophile **1**.

In contrast, a higher chemodivergent selectivity could be observed in a C-OTf selective functionalization in the presence of C-Cl bonds. Under standard reaction conditions monofunctionalization at the C-OTf site yielded thioether **3Fb** (70%) in a mixture with difunctionalized product (14%) and remaining starting material (16%). Additionally, chemoselective couplings of C-Cl (89%) and C-OTf (94%) bonds in the presence of tosylate substituent, which is relatively inert under the employed reaction conditions, generated the corresponding monothioether in excellent isolated yields. In these cases, the GC-FID analysis of the crude mixture was hampered by detectability of the substrates and monosubstituted products, but no disubstituted compound nor the product of single C-OTf sulfenylation were observed after isolation or on GC-MS. C-Cl selectivity in presence of C-OTf

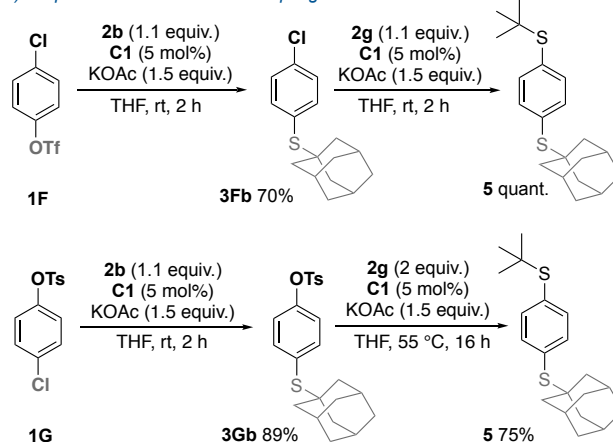
bonds is typical for Ni(0).¹⁶ The usefulness of the preferential activation of one particular C-X bond was further demonstrated in two sequential C-S couplings of biselectrophilic substrates **1F** and **1G** (Scheme 3b). Surprisingly, tosylate could be converted under higher temperature with longer reaction time. The sequence was also successfully performed in one-pot fashion for both substrates. No additional catalyst was needed in the second step.

Scheme 3. Intramolecular competitions of biselectrophiles and application in sequential transformation^a

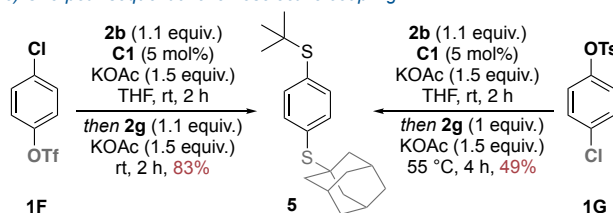
a) Intramolecular competition (1 equiv. of **1** + 1.1 equiv. of **2b**)

| | | | | | | |
|--------------------|------------------|------------------|------------------|------------------|-------------------|-------------------|
| | | | | | | |
| | Cl | Br | I | OTf | Cl | OTf |
| conv. 1 : | 67% | 68% | 63% | 84% | n.d. ^b | n.d. ^b |
| yield 3-X : | 34% | 43% | 53% | 70% | 89% ^c | 94% ^c |
| 3-Y : | 0% | 0% | 0% | 0% | 0% | 0% |
| 3-XY : | 33% ^d | 25% ^d | 10% ^d | 14% ^d | 0% | 0% |

b) Sequential chemoselective coupling



c) One-pot - sequential chemoselective coupling



^aGC-FID yields with pentadecane as internal standard, unless otherwise noted. ^bNot determined due to detection difficulties by GC-FID. ^cIsolated yields. ^dCalculated yields/GC-MS.

Next, we pursued mechanistic investigations of our catalytic reaction. Several experiments with radical scavengers (2 equiv.) were performed (see SI, Table S3). The reaction was suppressed in the presence of TEMPO (2,2,6,6-tetramethylpiperidinyloxy) and galvinoxyl radical, which are also known to react directly with Ni(0) species.¹⁷ On the other hand, the reactions with BHT (butylated hydroxytoluene) and 9,10-dihydroanthracene

proceeded smoothly, providing 82% and 85% yields of thioether product, respectively. These observations as well as the lack of paramagnetic signals in NMR experiments (Figures 3,4) lead to the assumption that a 2-electron mechanism with a Ni(0)/Ni(II) catalytic cycle is more likely. Cycles proceeding *via* alternative pathways, including single electron transfer steps cannot be ruled out completely, but they were not further considered.

In order to better understand the mechanism and the unique role the acetate plays,¹⁸ we performed DFT computations with the ORCA 4 electronic structure code.¹⁹ All structures were

optimized with the B3LYP(VWN-3) hybrid density functional²⁰ in combination with Grimme's D3-dispersion correction (with zero-damping)²¹ and a def2-SVP basis set,²² which treats all electrons explicitly (without an effective core potential). Furthermore, the electronic energies were refined by computing M06-L single point energies²³ with the prodigious def2-QZVPP basis set and solvation effects were accounted for implicitly using the SMD model²⁴ with THF as a solvent. Comparable levels of theory have previously been employed for the computational assessment of other Ni-catalyzed reactions.^{7b} The obtained results are displayed in Figure 1.

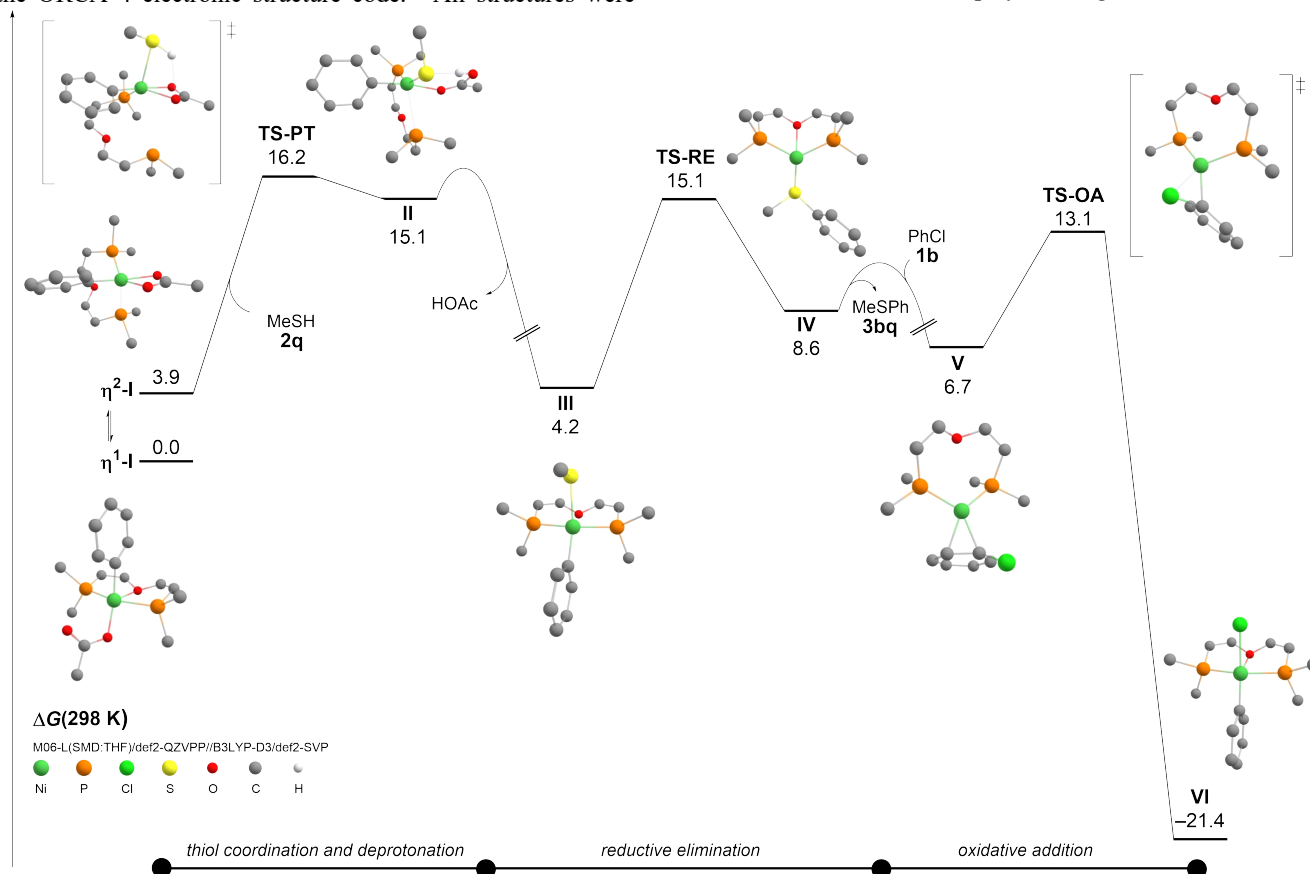


Figure 1. Free energy surface of the Ni-catalyzed cross-coupling reaction with methanethiol as a model nucleophile and chlorobenzene as the electrophile at the M06-L(SMD:THF)/def2-QZVPP/B3LYP-D3/def2-SVP level of theory. Only selected atoms of the Xantphos ligand are displayed and all carbon-bound hydrogens are omitted for clarity.

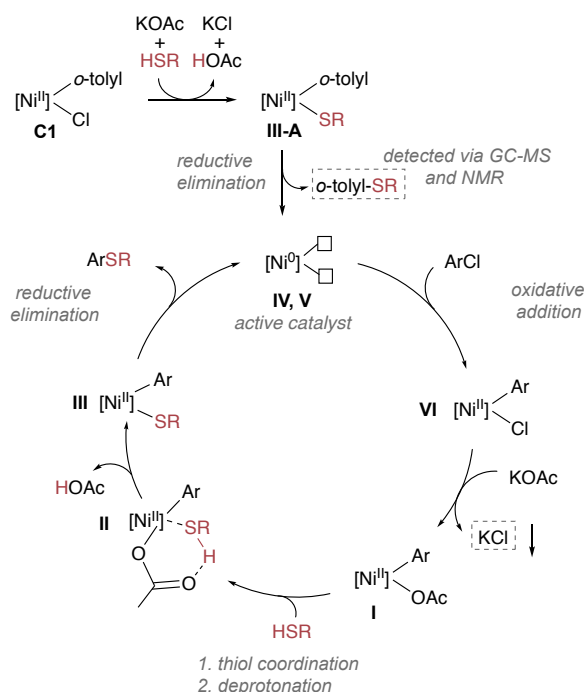
We were particularly interested in the role of the acetate both during the activation of the one-component Ni(II) precatalyst **C1** and during the active catalytic cycle. **C1** and the on-cycle oxidative addition product **VI** have a similar structural motive [LNi(II)ArCl], therefore activation of the catalyst and on-cycle catalysis share the same steps. Assuming the involvement of the metal during the deprotonation step and ligand exchange, Ni(II) complexes with acetate as a ligand were optimized.²⁵ Two isomeric complexes, η^1 -I and η^2 -I [LNi(II)ArOAc] were localized, in which the acetate acts as a mono- and bidentate ligand, respectively. The η^1 -I complex roughly assumes a distorted square-pyramidal geometry, in which both phosphorus atoms occupy equatorial positions across from each other at almost equal distances (~2.2 Å), while the oxygen atom of Xantphos sits in the apical position. In contrast, this oxygen atom is unbound in the 3.9 kcal mol⁻¹ less stable η^2 -I complex and one of the phosphorus donors is less tightly bound at a distance of 2.4 Å. This opens the possibility for the thiol

coupling partner to attack the metal center *trans* to the loosely bound phosphorus arm of the ligand. Using methanethiol as a model nucleophile, we were able to localize the transition state **TS-PT** at an energy of 16.2 kcal mol⁻¹. The reactive mode of the transition state mainly corresponds to a contraction of the Ni-S distance and an elongation of one of the Ni-O bonds to the acetate. As confirmed with the help of intrinsic reaction coordinate (IRC) computations, the reactive motion is consistent with an insertion of the SH-moiety into an Ni-O bond. However, we were unable to localize a minimum energy structure, in which the proton is still bound to the sulfur atom when thiolate and acetate are both coordinated to the nickel center suggesting that the transition state structure **TS-PT** corresponds to a metal-mediated proton transfer reaction. The resulting complex **II** is approximately square-planar and the second P-donor is remote from the coordination center (3.2 Å). Rebinding of the latter and dissociation of acetic acid in a not further elucidated order of events affords thiolate complex **III**

[LNi(II)ArSMe] at an energy of 4.2 kcal mol⁻¹. Therefore, the generation of thiolate complex **III** is modestly uphill but provides the possibility of product formation. The presumably interfering production of phenyl acetate by reductive elimination in **I** is not competitive since this process is associated with a prohibitive activation barrier of 44.0 kcal mol⁻¹. However, the reductive elimination of the thioether product **3bq** from complex **III** is activated by only 10.9 kcal mol⁻¹ in another uphill reaction step. The thioether is initially still bound to the resulting Ni(0) complex **IV**, but can be replaced by the chlorobenzene (**1b**). From there, facile oxidative addition under formation of complex **VI** provides sizable 28.1 kcal mol⁻¹ of driving force to the reaction. The generation of complex **I** from **VI** and potassium acetate is difficult to describe computationally since it might involve the precipitation of potassium chloride in a salt metathesis reaction.

The corresponding proposed catalytic cycle is depicted in Scheme 4. After activation of precatalyst **C1**, generation of the active Ni(0) species (shown without the coordinated electrophile) and oxidative addition of the aryl halide, the intermediate **VI** is formed. It further undergoes a ligand exchange with potassium acetate generating **I** and precipitating KCl via salt metathesis. Subsequent acetate promoted deprotonation of the metal pre-coordinated thiol leads to intermediate **II** [LNi(II)ArSR]. This step (via intermediate **II**) is analogous to the CMD (concerted metalation-deprotonation) mechanism occurring in C-H activation processes.²⁶ Finally, **III** undergoes reductive elimination to yield the product and to regenerate the active Ni(0) catalyst.

Scheme 4. Postulated mechanism via acetate-assisted catalysis



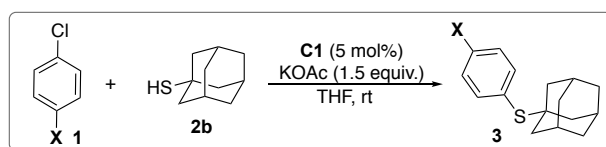
Several kinetic studies were conducted with electronic modifications of the electrophile (aryl chloride) and ligand, as well as steric modifications of the nucleophile (thiol) in order to analyze and compare initial periods, reaction rates and overall

yields. The reaction profiles of varying thiols are depicted within Table 4. Similar reaction rates for primary, secondary (both $k_{rel} = 0.95$) and tertiary thiols ($k_{rel} = 1.0$, see SI) indicate that the thiol is not relevant during the rate determining step or that its steric adaptations do not have any influence. However, a significantly longer initial period was observed for the tertiary thiol (1°: 2° = 5 min. 3° = 15 min.), which can be explained through the involvement of thiol during the activation of precatalyst **C1**. Due to the *ortho*-substituent on the aryl coordinated to nickel in **C1**, an increase in steric strain could disfavor the formation of **III-A** [LNi(II)ArSR], especially with a tertiary thiol. Low yield observed for the *ortho*-methyl substituted arylchloride **3rb**, in which the on-cycle intermediate **III** equals the activation intermediate **III-A** supports this theory.

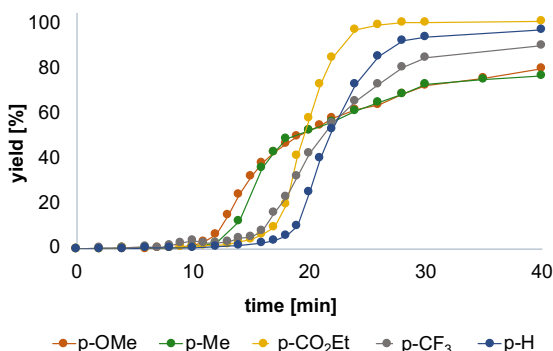
Another hint supporting the hypothesis that the activation of **C1** is responsible for an increase of the initial period is the use of Ni(cod)₂ and Xantphos as catalyst system, for which only a short induction period (< 2 min, Figure 2c in grey) was observed. The thiol is not involved in the in-situ generation of the active catalyst from a nickel(0) source.

In order to gain further insight into the mechanism and rate limiting step, Hammett studies were performed analyzing the influence of varying substituents on the ligand and electrophile on the reaction rate after the induction period (Figure 2, see SI section 6.1).²⁷ The series of experiments with modified aryl chlorides (*p*-OMe, *p*-Me, *p*-H, *p*-CO₂Et, *p*-CF₃) showed an impact of electronic properties on the reaction rate. Excluding the CF₃-substituent, a linear correlation with the σ_p Hammett constant was observed ($\rho = 0.46$, $R^2 = 0.96$) indicating that electron-withdrawing substituents increase the reaction rate to a specific point. The low ρ value is in agreement with the DFT calculation, indicating that the oxidative addition is not the rate determining step. However, the reaction rate decreased for highly electron deficient trifluoromethyl-substituted substrate ($\rho = -3.71$). This indicates a change in mechanism, the rate determining step or different overall contributions.

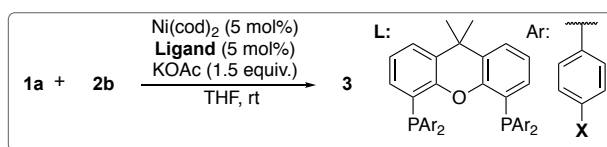
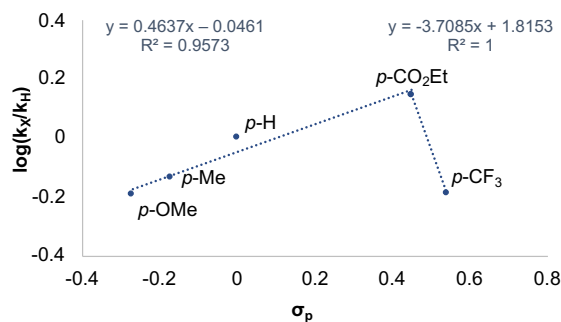
The second Hammett study included adaptations of the electronic properties of the Xantphos ligand (*p*-OMe, *p*-Me, *p*-H, *p*-CF₃), which were tested with Ni(cod)₂ as catalyst precursor *via* in-situ catalysis (Figure 2 c,d). Electron-donating substituents on the ligand increased the reaction rate ($\rho = 1.68$, $R^2 = 0.83$), but the *p*-CF₃-substituted ligand did not yield any product. Electron-donating ligands are known to stabilize higher oxidation states and promote the oxidative addition,²⁸ but the interpretation is complicated due to multiple factors. The reaction performed with defined catalyst **C1** is faster compared to the Xantphos/Ni(0) system. The lower reaction rate for Ni(cod)₂ can be explained by the presence of cod, which was found to suppress oxidative addition during catalysis by coordinating and stabilizing the active Ni(0) catalyst rendering it less reactive.^{7b, 29} Therefore the result of the Hammett analysis with Ni(cod)₂ as nickel source might not be completely adaptable to our catalytic system, as the additional cod might change rates of the elemental steps and disfavor the oxidative addition.



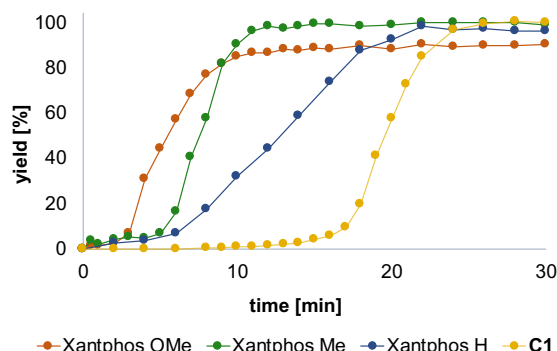
a) Arylchlorides: Kinetic Profiles



b) Arylchlorides: Hammett Analysis



c) Ligands: Kinetic Profiles



d) Ligands: Hammett Analysis

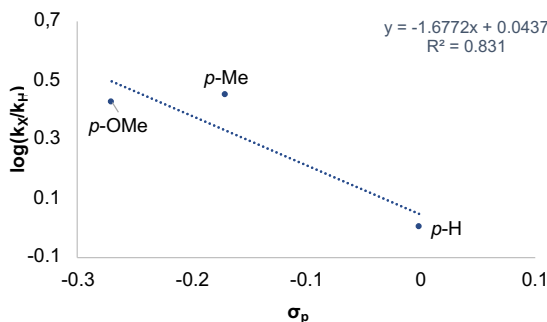


Figure 2. Kinetic and Hammett analysis. For reaction conditions, see SI.

To gain further insight into the mechanism, the standard reaction of **1a** with **2b** was followed by ³¹P{H} NMR (Figure 3, SI section 6.2). After 5 minutes, signals of the employed precatalyst **C1** (two different geometries, 6.55 and 1.43 ppm),¹⁰ free Xantphos (-18.20 ppm) and a new signal at 7.02 ppm were detected, which can be assigned to the oxidative addition intermediate **VI** [LNiArCl]. The signal could be reproduced by an isolated complex from a mixture of Ni(cod), Xantphos and **1a** (Figure 3-2). After about 30 minutes, two broad doublets appeared at 9.31 and 8.24 ppm, presumably the Ni(Xantphos)₂ complex. The signal was reproduced by the addition of Ni(cod)₂ and 2 equiv. of Xantphos (Figure 3-7). The complex has not yet been characterized in the literature, but it was previously identified as a catalyst sink.³⁰ Corresponding data for the analogous Pd complex is known from the literature and shows similar signals.³¹

Crystallization of the catalytic intermediates was not successful, yet. However, we were able to follow and compare the formation of a series of oxidative addition complexes **VI** [LNiArCl] in the catalytic transformation of three electron-poor aryl chlorides (Figure 4). Variation of para-substituents on the aryl chloride for the on-cycle generation of the oxidative addition product shows a shift in the ³¹P{H} signals correlating to the Hammett value (CO₂Et σ_p = +0.45, 7.02 ppm; CF₃ σ_p = +0.54, 7.47 ppm; SO₂Me σ_p = +0.73, 7.69 ppm). These signals could be reproduced in a reaction of Ni(cod)₂, Xantphos and the

corresponding aryl chloride. The experiments suggest that the oxidative addition product is the resting state of the catalytic cycle, which is in line with previous observations and our DFT computations. (for further NMR spectra, see SI section 6.2.).

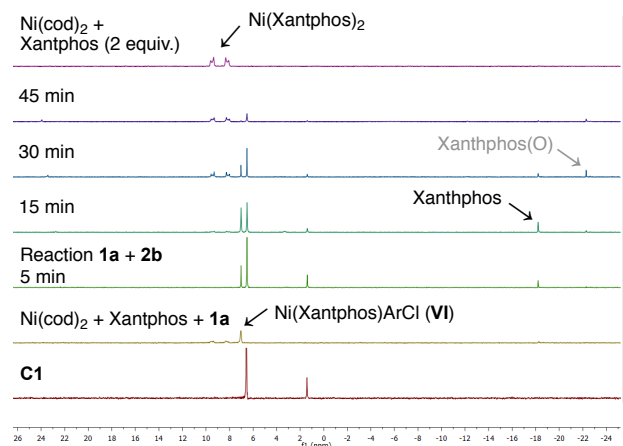


Figure 3. ³¹P{H} NMR spectra for the reaction progress of a standard reaction with **1a** and **3b** (3-6). With additional comparison spectra (1,2,7).

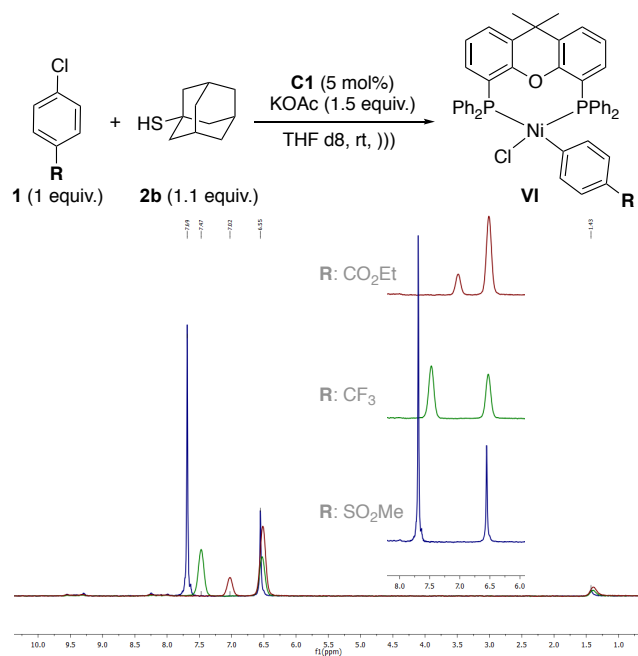


Figure 4. $^{31}\text{P}\{\text{H}\}$ NMR spectra of oxidative addition intermediates detected in the transformation of various electrophiles. Signals at 6.55 ppm and 1.43 ppm correspond to **C1**.

CONCLUSION

An operationally simple and mild nickel-catalyzed coupling of aryl chlorides with aliphatic thiols at room temperature was developed. Key feature is the combination of a defined air stable Ni(II) precatalyst and potassium acetate as base, without the need for further additives. A large variety of functional groups was tolerated, and complex pharmaceutically relevant compounds were functionalized. Chemoselective coupling of tertiary thiols with triflates in the presence of C-Cl and C-OTs bonds, as well as with chlorides in presence of C-OTs bonds was achieved. The conducted kinetic and NMR studies as well as DFT computations support a Ni(0)/Ni(II) catalytic cycle with the oxidative addition product as resting state and acetate playing a key role in the formation of a thiolate complex *via* internal deprotonation.

ASSOCIATED CONTENT

Supporting Information

The Supporting Information is available free of charge on the ACS Publications website.

General procedures, analytical data, NMR spectra (PDF), computational data.

AUTHOR INFORMATION

Corresponding Authors

* Ivana Fleischer: Institute of Organic Chemistry, Faculty of Science and Mathematics, Eberhard-Karls University Tübingen, Auf der Morgenstelle 18, 72076 Tübingen, Germany; ivana.fleischer@uni-tuebingen.de

* J. Philipp Wagner: Institute Organic Chemistry, Faculty of Science and Mathematics, Eberhard-Karls University Tübingen, Auf der Morgenstelle 18, 72076 Tübingen, Germany; philipp.wagner@orgchem.uni-tuebingen.de

Author Contributions

The manuscript was written through contributions of all authors. All authors have given approval to the final version of the manuscript.

ACKNOWLEDGMENT

We thank M. Abbas, A. Huber and S. Clewing for their synthetic contributions to the project during research internships and the analytics department of the University of Tübingen for their excellent work. Financial support from the University of Tübingen and FCI (Liebig Fellowship J. P. W.) is gratefully acknowledged. J. P. W. is grateful to Prof. Holger Bettinger for his generous support.

REFERENCES

- Migita, T.; Shimizu, T.; Asami, Y.; Shiobara, J.-i.; Kato, Y.; Kosugi, M., The Palladium Catalyzed Nucleophilic Substitution of Aryl Halides by Thiolate Anions. *Bull. Chem. Soc. Jpn.* **1980**, *53*, 1385-1389.
- (a) Scott, K. A.; Njardarson, J. T., Analysis of US FDA-Approved Drugs Containing Sulfur Atoms. *Top. Curr. Chem.* **2018**, *376*, 5; (b) Hill Jr., H. W.; Brady, D. G., Properties, environmental stability, and molding characteristics of polyphenylene sulfide. *Polym. Eng. Sci.* **1976**, *16*, 831-835; (c) Hilton, H. W.; Nomura, N. S.; Yauger, W. L.; Kameda, S. S., Absorption, translocation, and metabolism of metribuzin (BAY-94337) in sugarcane. *J. Agric. Food Chem.* **1974**, *22*, 578-582.
- For selected examples, see: (a) Li, G. Y., The First Phosphine Oxide Ligand Precursors for Transition Metal Catalyzed Cross-Coupling Reactions: C-C, C-N, and C-S Bond Formation on Unactivated Aryl Chlorides. *Angew. Chem. Int. Ed.* **2001**, *40*, 1513-1516; (b) Fernández-Rodríguez, M. A.; Shen, Q.; Hartwig, J. F., A General and Long-Lived Catalyst for the Palladium-Catalyzed Coupling of Aryl Halides with Thiols. *J. Am. Chem. Soc.* **2006**, *128*, 2180-2181; (c) Murata, M.; Buchwald, S. L., A general and efficient method for the palladium-catalyzed cross-coupling of thiols and secondary phosphines. *Tetrahedron* **2004**, *60*, 7397-7403.
- For selected examples, see: (a) Chekal, B.; Damon, D.; LaFrance, D.; Leeman, K.; Mojica, C.; Palm, A.; St. Pierre, M.; Sieser, J.; Sutherland, K.; Vaidyanathan, R.; Van Alsten, J.; Vanderplas, B.; Wager, C.; Weisenburger, G.; Withbroe, G.; Yu, S., Development of the Commercial Route for the Manufacture of a 5-Lipoxygenase Inhibitor PF-04191834. *Org. Process Res. Dev.* **2015**, *19*, 1944-1953; (b) Chekal, B. P.; Guinness, S. M.; Lillie, B. M.; McLaughlin, R. W.; Palmer, C. W.; Post, R. J.; Sieser, J. E.; Singer, R. A.; Sluggett, G. W.; Vaidyanathan, R.; Withbroe, G. J., Development of an Efficient Pd-Catalyzed Coupling Process for Axitinib. *Org. Process Res. Dev.* **2014**, *18*, 266-274.
- For selected reviews on nickel catalysis, see: (a) Ananikov, V. P., Nickel: The "Spirited Horse" of Transition Metal Catalysis. *ACS Catal.* **2015**, *5*, 1964-1971; (b) Tasker, S. Z.; Standley, E. A.; Jamison, T. F., Recent advances in homogeneous nickel catalysis. *Nature* **2014**, *509*, 299-309; (c) Diccianni, J. B.; Diao, T., Mechanisms of Nickel-Catalyzed Cross-Coupling Reactions. *Trends Chem.* **2019**, *1*, 830-844.
- (a) Kentaro, T., Nickel(0)-catalyzed Synthesis of Diaryl Sulfides from Aryl Halides and Aromatic Thiols. *Chem. Lett.* **1987**, *16*, 2221-2224; (b) Zhang, Y.; Ngew, K. C.; Ying, J. Y., The First N-Heterocyclic Carbene-Based Nickel Catalyst for C-S Coupling. *Org. Lett.* **2007**, *9*, 3495-3498; (c) Iglesias, M. J.; Prieto, A.; Nicasio, M. C., Well-Defined Allylnickel Chloride/N-Heterocyclic Carbene [(NHC)Ni(allyl)Cl] Complexes as Highly Active Precatalysts for $\text{C}\equiv\text{N}$ and $\text{C}\equiv\text{S}$ Cross-Coupling Reactions. *Adv. Synth. Catal.* **2010**, *352*, 1949-1954; (d) Martin, A. R.; Nelson, D. J.; Meiries, S.; Slawin, A. M. Z.; Nolan, S. P., Efficient C-N and C-S Bond Formation Using the Highly Active [Ni(allyl)Cl(IPr*OMe)] Precatalyst. *Eur. J. Org. Chem.* **2014**, *2014*, 3127-3131; (e) Cristau, H. J.; Chabaud, B.; Chêne, A.; Christol, H., Synthesis of Diaryl Sulfides by Nickel(II)-Catalyzed Arylation of Arenethiolates. *Synthesis* **1981**, *1981*, 892-894; (f) Talukder, M. M.; Miller, J. T.; Cue, J. M. O.; Udamulle, C. M.;

- Bhadran, A.; Biewer, M. C.; Stefan, M. C., Mono- and Dinuclear α -Diimine Nickel(II) and Palladium(II) Complexes in C–S Cross-Coupling. *Organometallics* **2021**, *40*, 83-94; (g) Yu, T.-Y.; Pang, H.; Cao, Y.; Gallou, F.; Lipshutz, B. H., Safe, Scalable, Inexpensive, and Mild Nickel-Catalyzed Migita-Like C–S Cross-Couplings in Recyclable Water. *Angew. Chem. Int. Ed.* **2021**, *60*, 3708-3713; (h) Liu, D.; Ma, H. X.; Fang, P.; Mei, T. S., Nickel-Catalyzed Thiolation of Aryl Halides and Heteroaryl Halides through Electrochemistry. *Angew. Chem. Int. Ed. Engl.* **2019**, *58*, 5033-5037.
7. (a) Jones, K. D.; Power, D. J.; Bierer, D.; Gericke, K. M.; Stewart, S. G., Nickel Phosphite/Phosphine-Catalyzed C–S Cross-Coupling of Aryl Chlorides and Thiols. *Org. Lett.* **2018**, *20*, 208-211; (b) Yin, G.; Kalvet, I.; Englert, U.; Schoenebeck, F., Fundamental Studies and Development of Nickel-Catalyzed Trifluoromethylthiolation of Aryl Chlorides: Active Catalytic Species and Key Roles of Ligand and Traceless MeCN Additive Revealed. *J. Am. Chem. Soc.* **2015**, *137*, 4164-4172; (c) Martín, M. T.; Marín, M.; Maya, C.; Prieto, A.; Nicasio, M. C., Ni(II) Precatalysts Enable Thioetherification of (Hetero)Aryl Halides and Tosylates and Tandem C–S/C–N Couplings. *Chem. Eur. J.* **2021**, *27*, 12320-12326.
8. Gehrtz, P. H.; Geiger, V.; Schmidt, T.; Srsan, L.; Fleischer, I., Cross-Coupling of Chloro(hetero)arenes with Thiolates Employing a Ni(0)-Precatalyst. *Org. Lett.* **2019**, *21*, 50-55.
9. (a) Guan, P.; Cao, C.; Liu, Y.; Li, Y.; He, P.; Chen, Q.; Liu, G.; Shi, Y., Efficient nickel/N-heterocyclic carbene catalyzed C–S cross-coupling. *Tetrahedron Lett.* **2012**, *53*, 5987-5992; (b) Xu, X.-B.; Liu, J.; Zhang, J.-J.; Wang, Y.-W.; Peng, Y., Nickel-Mediated Inter- and Intramolecular C–S Coupling of Thiols and Thioacetates with Aryl Iodides at Room Temperature. *Org. Lett.* **2013**, *15*, 550-553; (c) Venkanna, G. T.; Arman, H. D.; Tonzetich, Z. J., Catalytic C–S Cross-Coupling Reactions Employing Ni Complexes of Pyrrole-Based Pincer Ligands. *ACS Catal.* **2014**, *4*, 2941-2950; (d) Jouffroy, M.; Kelly, C. B.; Molander, G. A., Thioetherification via Photoredox/Nickel Dual Catalysis. *Org. Lett.* **2016**, *18*, 876-879; (e) Oderinde, M. S.; Frenette, M.; Robbins, D. W.; Aquila, B.; Johannes, J. W., Photoredox Mediated Nickel Catalyzed Cross-Coupling of Thiols With Aryl and Heteroaryl Iodides via Thiyl Radicals. *J. Am. Chem. Soc.* **2016**, *138*, 1760-1763; (f) Guo, F.-J.; Sun, J.; Xu, Z.-Q.; Kuhn, F. E.; Zang, S.-L.; Zhou, M.-D., C–S cross-coupling of aryl halides with alkyl thiols catalyzed by in-situ generated nickel(II) N-heterocyclic carbene complexes. *Catal. Commun.* **2017**, *96*, 11-14; (g) Jones, K. D.; Power, D. J.; Bierer, D.; Gericke, K. M.; Stewart, S. G., Nickel Phosphite/Phosphine-Catalyzed C–S Cross-Coupling of Aryl Chlorides and Thiols. *Org. Lett.* **2018**, *20*, 208-211; (h) Cavedon, C.; Madani, A.; Seeberger, P. H.; Pieber, B., Semiheterogeneous Dual Nickel/Photocatalytic (Thio)etherification Using Carbon Nitrides. *Org. Lett.* **2019**, *21*, 5331-5334; (i) Delcaillau, T.; Bismuto, A.; Lian, Z.; Morandi, B., Nickel-Catalyzed Inter- and Intramolecular Aryl Thioether Metathesis by Reversible Arylation. *Angew. Chem., Int. Ed.* **2020**, *59*, 2110-2114; (j) Rodriguez-Cruz, M. A.; Hernandez-Ortega, S.; Valdes, H.; Rufino-Felipe, E.; Morales-Morales, D., C–S cross-coupling catalyzed by a series of easily accessible, well defined Ni(II) complexes of the type [(NHC)Ni(Cp)(Br)]. *J. Catal.* **2020**, *383*, 193-198; (k) Talukder, M. M.; Miller, J. T.; Cue, J. M. O.; Udamulle, C. M.; Bhadran, A.; Biewer, M. C.; Stefan, M. C., Mono- and Dinuclear α -Diimine Nickel(II) and Palladium(II) Complexes in C–S Cross-Coupling. *Organometallics* **2021**, *40*, 83-94; (l) Isshiki, R.; Kurosawa, M. B.; Muto, K.; Yamaguchi, J., Ni-Catalyzed Aryl Sulfide Synthesis through an Aryl Exchange Reaction. *J. Am. Chem. Soc.* **2021**, *143*, 10333-10340.
10. Standley, E. A.; Smith, S. J.; Müller, P.; Jamison, T. F., A Broadly Applicable Strategy for Entry into Homogeneous Nickel(0) Catalysts from Air-Stable Nickel(II) Complexes. *Organometallics* **2014**, *33*, 2012-2018.
11. For catalysis using C1 catalyst, see: (a) Beattie, D. D.; Schareina, T.; Beller, M., A room temperature cyanation of (hetero)aromatic chlorides by an air stable nickel(II) XantPhos precatalyst and Zn(CN)₂. *Org. Biomol. Chem.* **2017**, *15*, 4291-4294; (b) Gehrtz, P. H.; Kathe, P.; Fleischer, I., Nickel-Catalyzed Coupling of Arylzinc Halides with Thioesters. *Chem. Eur. J.* **2018**, *24*, 8774-8778; for related Ni complexes, see: (c) McGuire, R. T.; Paffile, J. F. J.; Zhou, Y.; Stradiotto, M., Nickel-Catalyzed C–N Cross-Coupling of Ammonia, (Hetero)anilines, and Indoles with Activated (Hetero)aryl Chlorides Enabled by Ligand Design. *ACS Catal.* **2019**, *9*, 9292-9297; (d) Morrison, K. M.; McGuire, R. T.; Ferguson, M. J.; Stradiotto, M., CgPhen-DalPhos Enables the Nickel-Catalyzed O-Arylation of Tertiary Alcohols with (Hetero)Aryl Electrophiles. *ACS Catal.* **2021**, *11*, 10878-10884.
12. Brauer, D. J.; Krueger, C., Bonding of aromatic hydrocarbons to nickel(0). Structure of bis(tricyclohexylphosphine)(1,2- ϵ -2-anthracene)nickel(0)-toluene. *Inorg. Chem.* **1977**, *16*, 884-891.
13. Kalvet, I.; Guo, Q.; Tizzard, G. J.; Schoenebeck, F., When Weaker Can Be Tougher: The Role of Oxidation State (I) in P- vs N-Ligand-Derived Ni-Catalyzed Trifluoromethylthiolation of Aryl Halides. *ACS Catal.* **2017**, *7*, 2126-2132.
14. (a) Scattolin, T.; Senol, E.; Yin, G.; Guo, Q.; Schoenebeck, F., Site-Selective C–S Bond Formation at C–Br over C–OTf and C–Cl Enabled by an Air-Stable, Easily Recoverable, and Recyclable Palladium(I) Catalyst. *Angew. Chem. Int. Ed.* **2018**, *57*, 12425-12429; (b) Keaveney, S. T.; Kundu, G.; Schoenebeck, F., Modular Functionalization of Arenes in a Triply Selective Sequence: Rapid C(sp²) and C(sp³) Coupling of C–Br, C–OTf, and C–Cl Bonds Enabled by a Single Palladium(I) Dimer. *Angew. Chem. Int. Ed.* **2018**, *57*, 12573-12577.
15. (a) Reeves, E. K.; Entz, E. D.; Neufeldt, S. R., Chemodivergence between Electrophiles in Cross-Coupling Reactions. *Chem. Eur. J.* **2021**, *27*, 6161-6177; (b) Entz, E. D.; Russell, J. E. A.; Hooker, L. V.; Neufeldt, S. R., Small Phosphine Ligands Enable Selective Oxidative Addition of Ar–O over Ar–Cl Bonds at Nickel(0). *J. Am. Chem. Soc.* **2020**, *142*, 15454-15463.
16. Russell, J. E. A.; Neufeldt, S. R., C–O-Selective Cross-Coupling of Chlorinated Phenol Derivatives. *Synlett* **2021**, *32*, 1484-1491.
17. Greaves, M. E.; Ronson, T. O.; Lloyd-Jones, G. C.; Maseras, F.; Sproules, S.; Nelson, D. J., Unexpected Nickel Complex Speciation Unlocks Alternative Pathways for the Reactions of Alkyl Halides with dppe-Nickel(0). *ACS Catal.* **2020**, *10*, 10717-10725.
18. Kalek, M.; Jezowska, M.; Stawinski, J., Preparation of Arylphosphonates by Palladium(0)-Catalyzed Cross-Coupling in the Presence of Acetate Additives: Synthetic and Mechanistic Studies. *Adv. Synth. Catal.* **2009**, *351*, 3207-3216.
19. Neese, F., Software Update: the ORCA Program System, Version 4.0. *Wiley. Interdiscip. Rev. Comput. Mol. Sci.* **2018**, *8*, e1327.
20. (a) Becke, A. D., Density-Functional Thermochemistry. III. The Role of Exact Exchange. *J. Chem. Phys.* **1993**, *98*, 5648-5652; (b) Stephens, P. J.; Devlin, F. J.; Chabalowski, C. F.; Frisch, M. J., Ab Initio Calculation of Vibrational Absorption and Circular Dichroism Spectra Using Density Functional Force Fields. *J. Phys. Chem.* **1994**, *98*, 11623-11627.
21. Grimme, S.; Antony, J.; Ehrlich, S.; Krieg, H., A Consistent and Accurate Ab Initio Parametrization of Density Functional Dispersion Correction (DFT-D) for the 94 Elements H–Pu. *J. Chem. Phys.* **2010**, *132*, 154104.
22. Weigend, F.; Ahlrichs, R., Balanced Basis Sets of Split Valence, Triple Zeta Valence and Quadruple Zeta Valence Quality for H to Rn: Design and Assessment of Accuracy. *Phys. Chem. Chem. Phys.* **2005**, *7*, 3297-3305.
23. Zhao, Y.; Truhlar, D. G., A New Local Density Functional for Main-Group Thermochemistry, Transition Metal Bonding, Thermochemical Kinetics, and Noncovalent Interactions. *J. Chem. Phys.* **2006**, *125*, 194101.
24. Marenich, A. V.; Cramer, C. J.; Truhlar, D. G., Universal Solvation Model Based on Solute Electron Density and on a Continuum Model of the Solvent Defined by the Bulk Dielectric Constant and Atomic Surface Tensions. *J. Phys. Chem. B* **2009**, *113*, 6378-6396.
25. Li, Z.; Zhang, S.-L.; Fu, Y.; Guo, Q.-X.; Liu, L., Mechanism of Ni-Catalyzed Selective C–O Bond Activation in Cross-Coupling of Aryl Esters. *J. Am. Chem. Soc.* **2009**, *131*, 8815-8823.
26. For selected examples on CMD mechanism, see: (a) Stuart, D. R.; Fagnou, K., The Catalytic Cross-Coupling of Unactivated Arenes. *Science* **2007**, *316*, 1172-1175; (b) Gorelsky, S. I.; Lapointe, D.; Fagnou, K., Analysis of the Concerted Metalation-Deprotonation

- Mechanism in Palladium-Catalyzed Direct Arylation Across a Broad Range of Aromatic Substrates. *J. Am. Chem. Soc.* **2008**, *130*, 10848-10849; (c) Bugaut, X.; Glorius, F., Palladium-Catalyzed Selective Dehydrogenative Cross-Couplings of Heteroarenes. *Angew. Chem. Int. Ed.* **2011**, *50*, 7479-7481; (d) Zhang, S.; Shi, L.; Ding, Y., Theoretical Analysis of the Mechanism of Palladium(II) Acetate-Catalyzed Oxidative Heck Coupling of Electron-Deficient Arenes with Alkenes: Effects of the Pyridine-Type Ancillary Ligand and Origins of the meta-Regioselectivity. *J. Am. Chem. Soc.* **2011**, *133*, 20218-20229.
27. (a) Hansch, C.; Leo, A.; Taft, R. W., A survey of Hammett substituent constants and resonance and field parameters. *Chem Rev* **1991**, *91*, 165-195; (b) Hammett, L. P., The Effect of Structure upon the Reactions of Organic Compounds. Benzene Derivatives. *J. Am. Chem. Soc.* **1937**, *59*, 96-103.
28. Xiong, B.; Li, Y.; Wei, Y.; Kramer, S.; Lian, Z., Dual Nickel-/Palladium-Catalyzed Reductive Cross-Coupling Reactions between Two Phenol Derivatives. *Org. Lett.* **2020**, *22*, 6334-6338.
29. Bajo, S.; Laidlaw, G.; Kennedy, A. R.; Sproules, S.; Nelson, D. J., Oxidative Addition of Aryl Electrophiles to a Prototypical Nickel(0) Complex: Mechanism and Structure/Reactivity Relationships. *Organometallics* **2017**, *36*, 1662-1672.
30. Clevenger, A. L.; Stolley, R. M.; Staudaher, N. D.; Al, N.; Rheingold, A. L.; Vanderlinden, R. T.; Louie, J., Comprehensive Study of the Reactions Between Chelating Phosphines and Ni(cod)₂. *Organometallics* **2018**, *37*, 3259-3268.
31. Klingensmith, L. M.; Strieter, E. R.; Barder, T. E.; Buchwald, S. L., New Insights into Xantphos/Pd-Catalyzed C–N Bond Forming Reactions: A Structural and Kinetic Study. *Organometallics* **2006**, *25*, 82-91.
-